

The aspects of DMD pathology mitigated by the Jag1 OE in the week-old zebrafish larvae

INTRODUCTION

In Duchenne Muscular Dystrophy (DMD), muscle contraction initiates pathology that includes calcium persistence, cytoplasmic oxidative stress, and mitochondrial oxidative stress, as described in detail in previous chapters. Calcium, though essential to the very mechanism of contraction, is kept at low levels during rest, whereas transients of calcium influx and reabsorption are required for proper muscle function. The calcium persistence is likely due to the reduced activity of endoplasmic reticulum (ER) located calcium pump SERCA that reabsorbs calcium in an ATP-dependent manner (Duan et al., 2021). The mitochondria also contain several calcium channels to regulate calcium as several enzymatic reactions, especially the pyruvate dehydrogenase complex, are sensitive to calcium. The persistence of higher calcium affects mitochondrial energy generation (Rybalka et al., 2014) and increases mitochondrial ROS production (Hughes et al., 2019). In the cytoplasmic compartment, the calcium and ROS also have a positive feedback loop which is overactive in DMD (Mareedu et al., 2021). Hence, the calcium-activable proteases have been thought to initiate myofiber death via multiple mechanisms (Zablocka et al., 2021).

On the other hand, a master stress regulator in all cells – the p38MAPK is attributed to activating Bax-mediated apoptosis during the early stages of the disease (Wissing et al., 2014). In healthy contracting muscles, p38MAPK activation occurs via several mechanisms, resulting in PGC- α stability and activation (Fan et al., 2004). However, why p38MAPK activations turn pathological in dystrophic conditions is poorly understood. In later stages, most myofibers are lost by necroptosis due to a heightened immune response (Bencze, 2023). The inflammatory cytokines and their receptor-signaling has also been implicated in myofiber death. Nevertheless, pathology initiation in knockouts of these genes in mdx background (Giordano et al., 2015; Morgan et al., 2018; Sagheddu et al., 2018) suggests that inflammation is the most likely outcome of ongoing myofiber damage.

A recent study showed that myoblast proliferation and fusion during regeneration could also contribute to membrane damage seen in DMD, as mechanical properties of the membrane need

to change to allow myoblast fusion (Boyer et al., 2022). The immature regenerated myofibers are also considered a reason behind increased fragility. The activated satellite cells dividing asymmetrically and symmetrically express dystrophin transiently before generating committed myoblasts (Dumont et al., 2015; Feige et al., 2021). Hence, the absence of dystrophin can accelerate the loss of stem cells in two ways, more stem cells remain activated due to defects in asymmetric cell division (Chang et al., 2016) and need more activation due to damaged myofibers. Vieira and coworkers (2015) found a higher proliferation rate in myoblasts derived from "escaper" biopsy. However, it might not necessarily be a rescue mechanism as myoblast proliferation is already high in DMD patients. The single time point muscle biopsy from escapers does not resolve the difference in the rate of muscle damage or myogenic potential exhaustion seen in DMD.

We found that Jagged1 plasmid injection in the dystrophic larvae improved muscle structure and function, especially till 8-day age. Especially structurally, the decline between 4 and 8 days is not different. On the other hand, muscle function declined severely from 4 to 8 days of age in the dystrophic larvae, as mentioned in Chapter 3. Many therapies, like IGF, have improved muscle damage in patients however, the same failed to improve motor activity in patients (Rutter et al., 2020). The previous report on escaper GRMD mentioned increased fibrosis in the escapers which is usually considered pathological in DMD (Zucconi et al., 2010).

Additionally, improved survival and swimming speed at 4 dpf age in *Sapje* larvae with Jagged1 mRNA injection was also mentioned, but other aspects of pathology remain unexplored in this rescue (Vieira et al., 2015) Hence, we compared cytoplasmic and mitochondrial ROS in the dystrophic and rescued zebrafish larvae. Furthermore, the cell cycle analysis was also done to compare proliferating and apoptotic cells in the larval tails, as muscle forms 80% of tissue in larval tails. In addition, we further checked the differential expression of canonical Notch target genes to elucidate the downstream effectors' involvement in the rescue.

MATERIALS AND METHODS

All the experiments were done on 8 dpf larvae as it represents a later stage of disease progression, and more tissue is available for analysis.

CYTOPLASMIC ROS QUANTIFICATION

The cell-permeable reagent 2',7'-dichlorofluorescein diacetate (DCFDA, also known as H2DCFDA, DCFH-DA, and DCFH) is helpful in quantitatively assessing reactive oxygen

species (ROS) in live cell samples. It measures hydroxyl, peroxy and other ROS activity within the cell. After absorption in cells, H2-DCFDA is then deacetylated by cellular esterases to a non-fluorescent compound, which ROS can oxidize into 2', 7'-dichlorofluorescein (DCF). DCF is highly fluorescent and is detected by fluorescence spectroscopy with excitation/emission at 485 nm /535 nm. Five larvae from each injection group were taken. The DCFDA dye was added at a final concentration of 1.8 μ M and incubated in the dark for 20 mins, and then washed with PBS three times in the dark and imaged under a fluorescent confocal microscope. The fluorescence intensities were calculated by Image J software as arbitrary units (a.u.) from a single larval tail. Group mean and SD of 3 larvae was used for a single replicate.

MITOCHONDRIAL ROS QUANTIFICATION

JC-1 is a lipophilic cationic carbocyanine dye that accumulates in mitochondria. It emits a red fluorescence at 590nm in dimeric form. In the monomeric form, it emits green fluorescence at 488nm. When there is high oxidative stress in mitochondria, it reacts with this dye, causing its monomerization and increasing green emission. The ratio of Red/Green emission is taken into consideration to assess mitochondrial membrane potential and thus health in any disease condition. The absorption significantly reduces after 4 dpf in larvae, therefore, in vivo mitochondrial membrane potential measurements directly from muscles under a confocal microscope were unsuccessful. Hence Red and Green emissions were measured on larval muscle suspensions by Fluorescence Activated Cell Sorter (FACS). Ten larvae from each injection group were quickly euthanized in cold water. Only tails were cut from the larvae and collected for analysis. These were digested in trypsin EDTA (1X) and Collagenase IV (1mg/ml) for 5 mins. The CO₂-free complete media was used to neutralize the enzymes (trypsin and collagenase IV) and reduce the stress of cells in single-cell suspension. The JC1 dye was added to this media at 5 μ M final concentration for 10 minutes, and emission was measured in a BD Accuri™ C6 Plus Flow Cytometer. The data acquired were analyzed using BD Accuri™ software and GraphPad Prism software to generate graphs.

CELL CYCLE ANALYSIS BY PROPIDIUM IODIDE STAINING

Propidium iodide (PI) the intercalating agent is not permeable to live cells. It is absorbed only by dead cells. Once inside cells, it binds to DNA by intercalating between the nitrogen bases. Once it binds to DNA, it is stable and emits red fluorescence, which can be assessed by fluorescent microscopy or FACS. In FACS, the inherent properties of cells and nucleus to diffract the light captured as forward and side scatter depend on the size and content of

cytoplasm and nucleus. The cell cycle analysis was carried out on BD Accuri™ FACS machine based on PI staining in fixed cells. In the present study, five larvae from each group were fixed in 4% PFA overnight at 4°C. The head and fat pouches were cut off. Then larvae tails were digested with trypsin and collagenase-IV for 5 mins at 37°C. The digestion was stopped by washing three times with PBS. Further, by pipetting, the tissue in the suspension was disrupted. This suspension was passed through a 45 µm membrane filter to remove debris. The single-cell suspension was treated with 30-40 µM PI final concentration for 20 mins in the dark and used for cell cycle analysis.

The RNA isolation, cDNA synthesis, and real-time PCR of zebrafish Notch targets (primers mentioned in Chapter 2) were done for DCFDA individual larval tails and were imaged following DCFDA staining. Samples pooled from 3-5 larval tails were used for Real-time PCR, Cell cycle analysis and mitochondrial membrane potential with the help of FACS. The results are expressed as Mean ± SD. The two-way ANOVA followed by Tukey's multiple comparisons was done in GraphPad Prism software. A p-value of ≤0.05 is considered significant.

RESULTS

JAGGED1 OVEREXPRESSION REDUCES CYTOPLASMIC OXIDATIVE STRESS IN DYSTROPHIC ZEBRAFISH LARVAE.

The intensity of this fluorescence (arbitrary units) is taken as a measure of oxidative stress. As Figure 4.1A shows, oxidative stress is higher in the DMD group than Control but reduces with Jagged1 OE, as seen in the rescue group. The fluorescence intensity from stained larval tail muscles of the DMD group (122.8 ± 31.44) was higher than the control group (112 ± 21.09) though not significant statistically. The rescue group showed a statistically significant reduction in intensity (80 ± 15.63) compared to DMD (p-value 0.032) (Table 4.1).

JAGGED1 OVEREXPRESSION INCREASES MITOCHONDRIAL ROS PRODUCTION DURING RESCUE

Figure 4.2A shows how gating was applied to JC-1 stained cells from which data was obtained. The ratio of green/red percentage cells from the population was calculated using Microsoft Excel. The statistical analysis, which is given in Figure 4.2B, shows a higher green/red ratio in the rescue group (8.81 ± 3.44) as compared to Control (1.14 ± 0.032) and DMD (2.22 ± 0.064) groups. In the control background as well, Jag1 overexpression increases mitochondrial ROS production, however, this effect seems more pronounced in the dystrophic condition (Table 4.2).

JAGGED1 OVEREXPRESSION REDUCES THE PERCENTAGE OF APOPTOTIC CELLS AND INCREASES THE PROLIFERATING CELLS

Figure 4.3A shows representative graphs of FACS gating used to quantify percent cell populations in different cell cycle stages. The M4 gate shows apoptotic cells, whereas M1, M2, and M3 represent the G0/G1, S, and G2/M phases of the cell cycle (Table 4.3). Only apoptotic and dividing cell percentages were compared between the control, DMD and DMD+Jag1 (rescue) groups. The statistical analysis shows that the percent apoptotic cells are higher in the DMD (8.95 ± 1.89) compared to Control (4.41 ± 1.53) which is reduced in the rescue group (5.75 ± 1.13) (Figure 4.3B). There was also a trend of increase in the G2/M percent population in the rescue compared to the Control and dystrophic (Figure 4.3C), although statistically non-significant (Table 4.4).

THERE IS A NON-SIGNIFICANT INCREASE IN SOME CANONICAL NOTCH TARGET GENES IN DYSTROPHIC AND RESCUE LARVAE

To narrow down the possible downstream effectors of this rescue, the transcription levels of canonical notch target genes were quantified by real-time polymerase chain reaction. Figure 4.4 shows that all tested notch target genes are already upregulated in DMD condition and further upregulated by the Jag1 overexpression, except Her9. The Jag1 overexpression in the control background showed several-fold upregulation of notch target genes, but errors were too high (data not shown here). This differential gene expression (DGE) data remained statistically non-significant as variability was very high and taken from only two replicates.

DISCUSSION

The muscle activity-associated processes like calcium ingress, Na^+/H^+ exchanger activity, and oxidative stress turn pathological in dystrophic conditions. Activation of master stress regulator p38MAPK also causes apoptosis (Wissing et al., 2014) instead of usual PGC1- α activation for metabolic adaptation in healthy muscles in response to exercise (Fan et al., 2004). Thus, dystrophic muscles' inherent poor stress response at structural, osmotic, signaling, and metabolic levels results in perpetual damage during low-intensity daily activity in patients. The damage-activated immune response is also required for proper regeneration in healthy muscles, but DMD does not reach the resolution phase due to ongoing damage. The continuous cycles of degeneration-regeneration and heightened inflammatory milieu cause exhaustion of myogenic potential at a young age (Blau et al., 1983), making disease progression non-reversible.

As reported previously by Duan et al., (2021), we found a higher percentage of dying cells in addition to increased cytoplasmic and mitochondrial oxidative stress in dystrophic larval tail muscles. There is a significant reduction in dividing cells from the dystrophic larval tail. In zebrafish (Sapje and Sapje-like) models of DMD, damage by 3-4 days post-fertilization (dpf) and regeneration during 4-10 dpf has been shown (Berger et al., 2010; Seger et al., 2011). The larval tail is composed of 80% of muscles, while a small percentage of other cells comprise the rest. The immune and endothelial cells are expected to have higher proliferating cells in the inflammatory condition of dystrophy. Hence, the steep reduction of proliferating cells found in dystrophic larval tails in the present study (Figure 4.3A) probably depicts a loss of myogenic potential at 8 days of age. The rescue group shows a significantly higher percentage of proliferating cells than the dystrophic and Control groups (Figure 4.3B). This correlates with preserving myogenic potential from original “escaper” GRMDs (Vieira et al., 2015), suggesting rescuing mechanism is conserved. The higher percentage of cells in the S-phase can also indicate a hindrance to cell cycle progression. It has been shown that Jagged1 expression in patient-derived myoblasts interferes with the mitogenic action of IL-1 β (Nagata et al., 2017). Cell cycle inhibition can induce apoptosis in proliferating cells, but the reduction in apoptotic cells in the rescue group does not support this possibility. Moreover, increased myoblast death during regeneration would result in disease exacerbation, not the functional rescue reported in the “escaper” GRMD or 8-day-old zebrafish larvae we observed (chapter 4). One drawback in this study is the lack of myoblast-specific antibodies, which would have confirmed the identity of cells in apoptotic and proliferating populations.

The decrease in the fluorescence intensity of DCF indicates reduced cytoplasmic oxidative stress in the rescue group compared to the dystrophic group (Figure 4.1). Though the role of oxidative stress in pathogenicity is known in great detail, antioxidants like N-acetyl Cysteine (NAC), glutathione supplementation, or selenium which improves glutathione assimilation, are not found to improve the patient’s condition (Guiraud and Davies, 2017). One of the master transcriptional regulators of oxidative stress response NRF2, when knocked out in heterozygous condition (NRF2^{-/+}), did not exacerbate injury in mdx background (Bronisz-Budzyńska et al., 2020). This indicates that, instead, ROS production is more likely pathogenic in DMD than a poor response to oxidative stress. However, activators of NRF2 are being tested in the *mdx* model (Kourakis et al., 2021). Studies from different cancers suggest that Notch signaling helps survive oxidative stress (Kumar et al., 2022), especially in progenitor cells independently of NRF or AP1 (Packer et al., 2020). Notch intracellular domain (NICD) also has been shown to

bind and inhibit an apoptotic effector called ASK1 downstream of p38MAPK signaling (Mo et al., 2013). Hence, there are several mechanisms by which Jag1-Notch signaling can reduce oxidative stress in dystrophic muscles, but to decipher the exact mechanism requires further study.

In addition to sarcolemma-associated NOC and Xanthine Oxidase (XO), mitochondria are considered a significant source of ROS in DMD. The persistence of calcium or cytoplasmic oxidative stress is thought to cause increased mitochondrial ROS production (Rybalka et al., 2014; Hughes et al., 2019). Dystrophic mitochondria also consume 50% less oxygen during rest and exercise, which results in half of ATP production compared to healthy muscles (Liang, 1986; Chinet et al., 1994; Kuznetsov et al., 1998; Rybalka et al., 2014). The reduced activity of complex-I of the electron transport chain (ETC) is thought to be the reason behind increased ROS production and reduced ATP production (Rybalka et al., 2014). Though overactive Uncoupling Protein-2 (UCP-2) shunting electron potential towards heat production (Markham et al., 2017) and accumulated α -ketoglutarate inhibiting ATP Synthase (Chin et al., 2014) also contribute to lower ATP production from dystrophic mitochondria (Timpani et al., 2015). It is unknown whether mitochondrial ROS production is causal in lower ATP synthesis or the result of lower TCA, ETC in the case of DMD. Here, unexpectedly we find increased mitochondrial ROS production in the rescue group compared to Control or DMD group. Given the known severe energy starvation in the dystrophic muscles, and the structural-functional rescue seen at 8 dpf larvae (chapter 4), it is very likely that, this increased ROS is linked to increased mitochondrial ATP production but needs further confirmatory study. The increased ROS production could also increase fibrosis via inflammatory modulation (Reid & Alexander, 2021), though not checked here, as described in the “escaper” GRMD muscles (Zucconi et al., 2010).

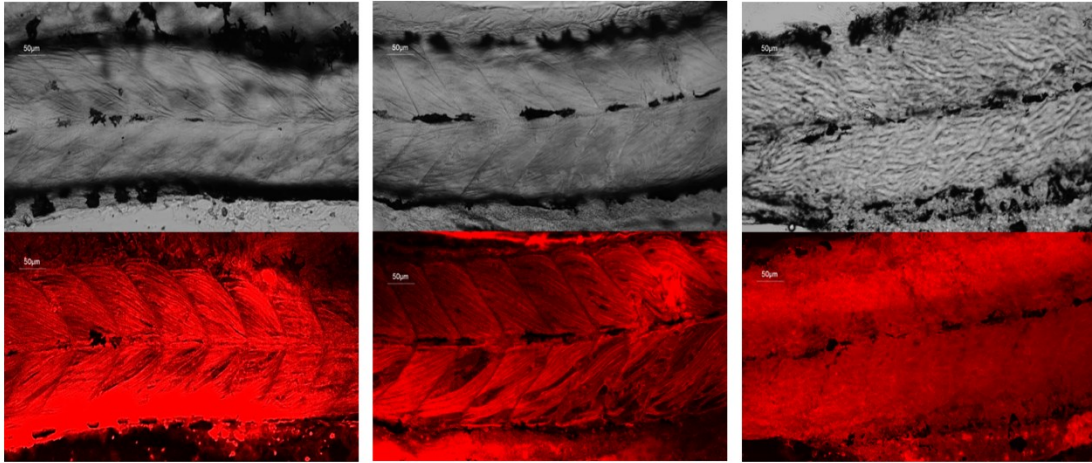
Real-time PCR data did not reveal any significant upregulation of Notch target genes, which could be due to the lesser number of experimental replicates used here. The Notch receptor activation and the target gene expression are transient events that last only 6-10 hours after stimulation by the ligand. The way this study was designed, there is no way to predict when Jagged1 would activate the notch receptors and in which tissue. Hence, it remains inconclusive as to which downstream effectors are involved in this rescue. The *in vitro* cultures are a more feasible option to manipulate this pathway during the myogenin (MyoG) expression window in

muscles without off-target tissue involvement. Such experiments carried out on patient-derived myoblast cultures are described in the next chapter (chapter 5).

CONCLUSION

The Jagged1 overexpression changes several pathological processes in the dystrophic background. These results suggest that Jagged1-mediated rescue involved lower cytoplasmic ROS production and higher mitochondrial ROS, which could be a reason behind reduced apoptotic cells. The reduced cell population in the S phase likely indicates the exhaustion of the myogenic progenitor pool in the dystrophic larvae. The rescue very likely involves the preservation of the myogenic potential, though it could not be ascertained whether rescued larvae had more progenitor pool from the beginning or not. The downstream effectors could not be ascertained in the zebrafish model of DMD in the present study. The Jagged1-Notch pathway is pleiotropic, likely mitigating these pathological processes via multiple effectors. The exact consequence of Jagged1 overexpression in the muscle and myogenin window can shed further light on the mechanism and is probed in the next chapter.

A



B DCFDA STAINING FOR OXIDATIVE STRESS

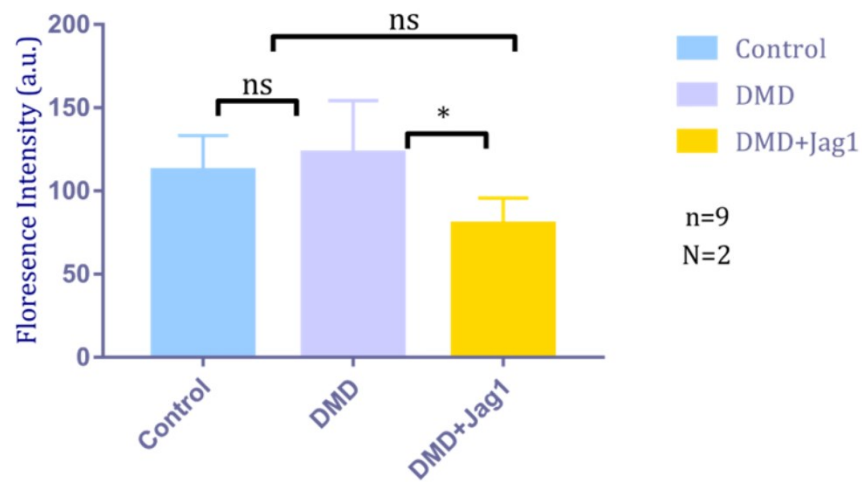


Figure 4.1: Cytoplasmic ROS quantification. A: Representative images of bright-field and corresponding DCFDA stained images of Control, DMD, and DMD+Jag1(rescue) group; B: Graph showing statistical analysis of Florescence Intensity following DCFDA staining in Control (112 ± 21.09), DMD (122.8 ± 31.44) and DMD+Jagged1 (80 ± 15.63).

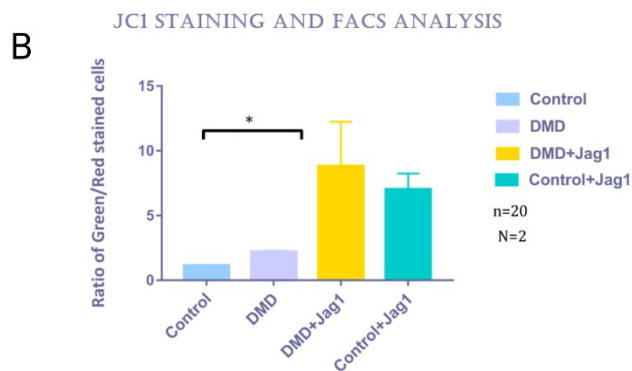
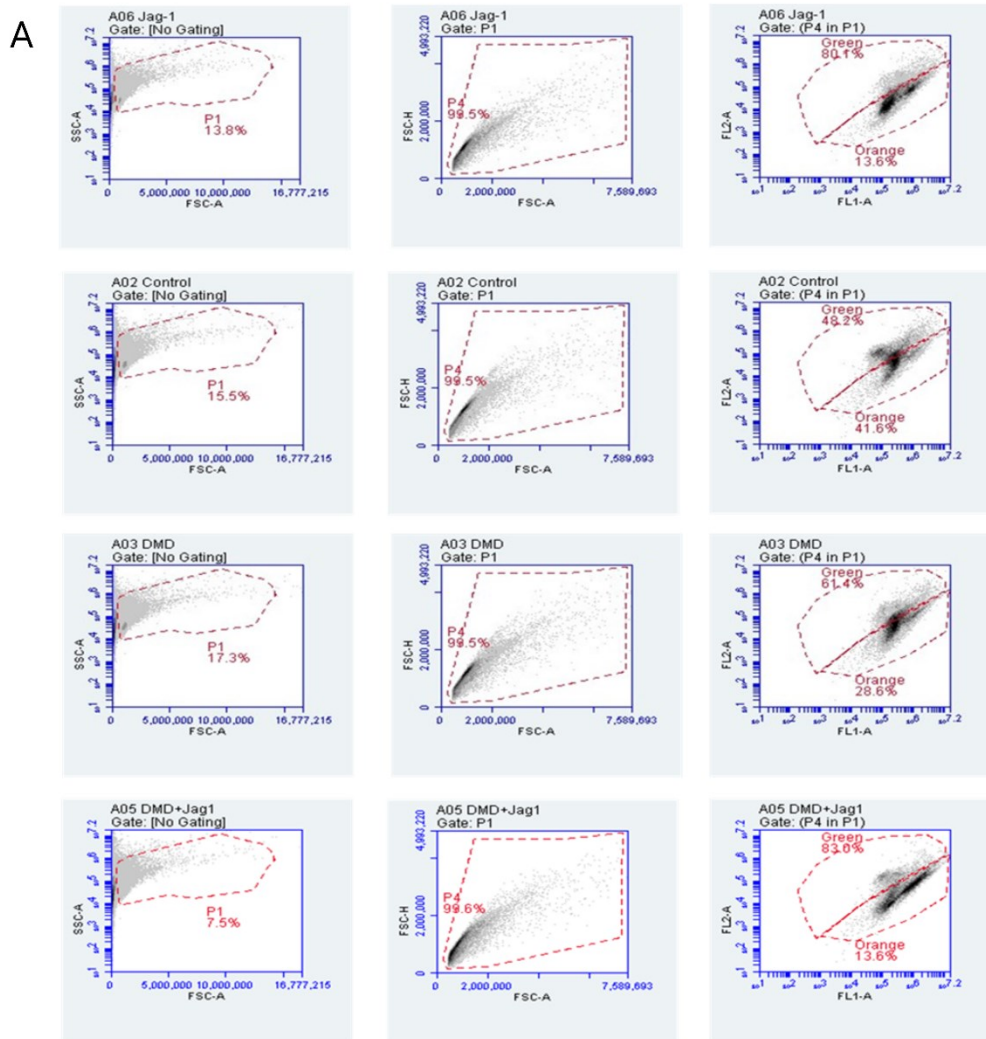


Figure 4.2: JC1 dye staining for Mitochondrial ROS with FACS. A: Representative images showing gating applied to quantify the ratio of green/red fluorescent emitting percent of cells from larva; tail; B: graph showing statistical analysis of ratio in Control (1.14 ± 0.032), DMD (2.22 ± 0.064) and DMD+Jagged1 (8.81 ± 3.44).

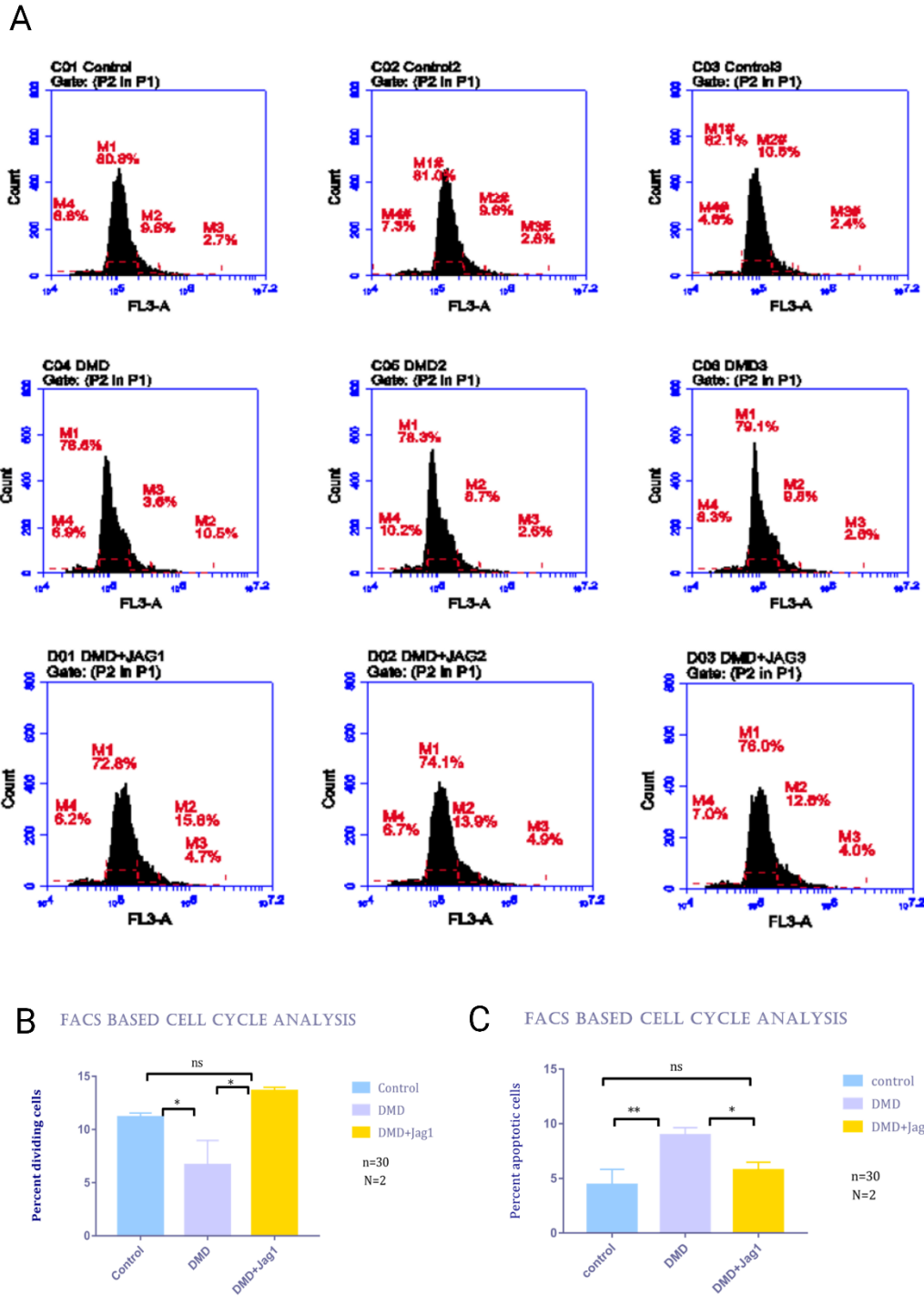


Figure 4.3: The cell cycle analysis of larval tail tissue. A: representative FACS graphs showing cell population in M4-apoptotic stage, M1-G0/G1, M2-S-phase, M3-G2/M stage after gating; B: graph of statistical analysis of Percent Apoptotic Cells; C: graph of statistical analysis of Percent Dividing cells in S-phase.

NOTCH TARGET GENE EXPRESSION

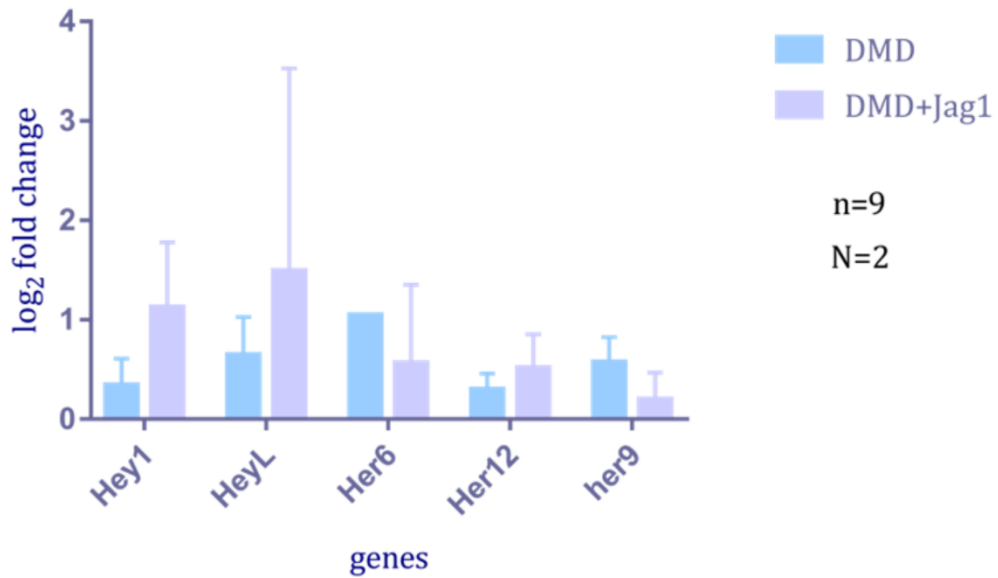


Figure 4.4: Real-time PCR of Notch Target Genes. A: Graph showing Real-Time PCR quantification of Notch Targets (Hey1, HeyL, Her6, Her12, Her9) from 2 replicates do not show statistically significant genes differentially expressed between Control, DMD, and DMD+Jagged1 groups.

Table 4.1: Quantification of DCFDA Staining for Oxidative Stress in larval tail.

Group	Fluorescence Intensity (a.u.)
Control	112±21.09
DMD	122.8± 31.44
DMD + Jagged1	80±15.63

Table 4.2: Percent cell population showing green/red fluorescence in larval tail using JC1 Stain.

Group	Ratio of green/red fluorescent emission
Control	1.14±0.032
DMD	2.22±0.064
DMD + Jagged1	8.81±3.44

Table 4.3: Percent apoptotic cell population from larval tissue using PI Staining.

Group	% of Dividing Cells
Control	11.15±0.41
DMD	6.667±2.297
DMD + Jagged1	13.63±0.033

Table 4.4: Percent apoptotic cell population from larval tissue using PI Staining.

Group	% of Apoptotic cells
Control	4.41±1.53
DMD	8.95±1.89
DMD + Jagged1	5.75±1.13